TASI 2016 notes, Sally Dawson

This is a draft. Please send suggestions for improvements to dawson@bnl.gov. I haven't put in references, so don't bother sending those. I'll get around to it soon.

I. INTRODUCTION TO THE SM

Introduction and SM discussion coming soon

A. Computing the ρ Parameter in a model with a Scalar Triplet

The result $\rho = 1$ is a result of an approximate global symmetry of the SM known as custodial symmetry. Remember that in the SM,

$$M_W = \frac{gv}{2} \tag{1}$$

$$M_Z = \sqrt{g^2+g'^2}\frac{v}{2}, \tag{2}$$

implying that there is a symmetry when $g' \to 0$, that results in $M_W = M_Z$. In this limit there is a rotation symmetry $W^1 \leftrightarrow W^2 \leftrightarrow W^3$. This symmetry is broken by the gauging of hypercharge and is known as custodial symmetry. Remember that,

$$\sin\theta_W = \frac{g'}{\sqrt{g^2+g'^2}}, \tag{3}$$

and so $g' \to 0$ corresponds to the limit $\cos\theta_W \to 1$.

Now add a real scalar triplet with $Y = 0$. It cannot give mass to charged fermions because there are no $SU(2)\times U(1)$ invariant couplings. The triplet does, however, contribute to gauge boson masses. The $SU(2)$ generators for a triplet can be written as,

$$J_1 = \frac{1}{\sqrt{2}}\begin{pmatrix} 0 & 1 & 0 \\ 1 & 0 & 1 \\ 0 & 1 & 0 \end{pmatrix} \qquad J_2 = \frac{i}{\sqrt{2}}\begin{pmatrix} 0 & -1 & 0 \\ 1 & 0 & -1 \\ 0 & 1 & 0 \end{pmatrix} \qquad J_3 = \begin{pmatrix} 1 & 0 & 0 \\ 0 & 0 & 0 \\ 0 & 0 & -1 \end{pmatrix}, \tag{4}$$

and the real triplet scalar is,

$$P = \begin{pmatrix} \eta^+ \\ \eta^0 + v' \\ \eta^- \end{pmatrix}. \tag{5}$$

We note that the assignment of charges in Eq. 5 satisfies $QP \sim (J_3 + Y)P$ and assures that the vacuum expectation value does not break electric charge.

Remember that the coupling of the $U(1)$ gauge boson is proportional to Y, so P does not couple to B. Now write the kinetic energy term as,

$$Ł \sim \frac{1}{2}(D_\mu P)^\dagger (D^\mu P)\,, \tag{6}$$

and the covariant derivative can be expanded,

$$\begin{aligned} D_\mu &= \partial_\mu + ig' B_\mu Y + igJ^i W^i_\mu \\ &\to \partial_\mu + \frac{ig}{\sqrt{2}} \begin{pmatrix} \sqrt{2}W_3 & W_1 - iW_2 & 0 \\ W_1 + iW_2 & 0 & W_1 - iW_2 \\ 0 & W_1 + iW_2 & -\sqrt{2}W_3 \end{pmatrix} . \end{aligned} \tag{7}$$

The triplet generates mass terms,

$$M_W = gv' \tag{8}$$

$$M_Z = 0\,. \tag{9}$$

So in the limit $g' \to 0$, P does not generate the same masses for W and Z. There is a symmetry $W^1 \leftrightarrow W^2$, but not the full custodial symmetry.

II. W AND Z GAUGE BOSONS AND THE HIGGS

We return to the kinetic energy term for the Higgs boson after electroweak symmetry breaking,

$$(D_\mu \Phi)^\dagger (D^\mu \Phi) \to \frac{1}{2}\left[\frac{g^2}{2} W^+_\mu W^{\mu -} (v + H)^2 + \frac{g^2}{4c_W^2} Z_\mu Z^\mu (v + H)^2\right], \tag{10}$$

and we note that the Higgs always appears in the combination $(h + v)^2$. Consider for a minute a Higgs boson heavy enough to decay to 2 physical W's and compute the decay $H \to W^+W^-$,

$$A^{\mu\nu}(H \to W^+W^-) = igM_W \epsilon^\mu(p_{W+})\epsilon^\nu(p_{W-})\,, \tag{11}$$

where $\epsilon(p_W)$ are the polarization vectors of the W bosons and satisfy the polarization sum rule,

$$\Sigma_{polarizations} \epsilon^\mu(p_{W1})\epsilon^\nu(p_{W2}) = -g^{\mu\nu} + \frac{p^\mu_{W1} p^\nu_{W2}}{M_W^2}\,. \tag{12}$$

Summing over the polarizations,

$$\Gamma(H \to W^+W^-) = \frac{\sqrt{1-4M_W^2/M_H^2}}{16\pi M_H}\frac{g^2M_H^4}{4M_W^2}\left(1-4\frac{M_W^2}{M_H^2}+12\frac{M_W^4}{M_H^4}\right). \tag{13}$$

The growth with M_H^4 is a manifestation of the longitudinal W modes. The interesting physics is in the longitudinal sector, where to leading order,

$$\epsilon_L(p_W) = \frac{1}{M_W}(\mid \vec{p_W} \mid, 0, 0, E_W) \sim \frac{p_W}{M_W} + \mathcal{O}\left(\frac{M_W^2}{E^2}\right). \tag{14}$$

Eq. 11 becomes in this limit,

$$A^{\mu\nu}(H \to W_L^+W_L^-) \to ig\frac{p_{W2}^\mu p_{W2}^\nu}{M_W}\,, \tag{15}$$

and the first term in the parenthesis of Eq. 13 is obtained.

One interesting consequence of Eq. 14 is that at leading order in M_W/E, longitudinal W's don't couple to massless fermions. With the physical mass of the Higgs boson, $M_H = 125\ GeV$, the Higgs cannot however decay into 2 real W's, but decays into one real and one virtual W which then decays to all of the allowed fermion pairs.

A. Unitarity

Contributions from dimension -6 EFT operators generate a dependence on s/Λ^2, which at high energy can become large. Cross sections rising with s will eventually violate perturbative unitarity, a simple result derived very generally from the optical theorem. To see this we consider $2 \to 2$ elastic scattering, where the differential cross section can be written as,

$$\frac{d\sigma}{d\Omega} = \frac{1}{64\pi^2 s} \mid A \mid^2 . \tag{16}$$

Using a partial wave decomposition,

$$A = 16\pi \sum_{l=0}^{\infty}(2l+1)P_l(\cos\theta)a_l \quad , \tag{17}$$

where a_l is the spin l partial wave and $P_l(\cos\theta)$ are the Legendre polynomials. The cross section becomes,

$$\begin{aligned}\sigma &= \frac{8\pi}{s}\sum_{l=0}^{\infty}\sum_{l'=0}^{\infty}(2l+1)(2l'+1)a_l a_l^* \\ &\qquad \cdot \int_{-1}^{1} d\cos\theta P_l(\cos\theta)P_{l'}(\cos\theta) \\ &= \frac{16\pi}{s}\sum_{l=0}^{\infty}(2l+1) \mid a_l \mid^2 \quad ,\end{aligned} \tag{18}$$

where we have used the fact that the P_l's are orthogonal. The optical theorem gives,

$$\sigma = \frac{1}{s} Im\Big[A(\theta = 0)\Big] = \frac{16\pi}{s} \sum_{l=0}^{\infty} (2l+1) \mid a_l \mid^2 . \tag{19}$$

This immediately yields the unitarity requirement

$$\mid Re(a_l) \mid < \frac{1}{2} , \tag{20}$$

which requires that there be no terms that grow with energy, as they will eventually violate the bound, at which point the theory becomes non-perturbative.

B. $W^+W^- \to W^+W^-$

As an example of the power of unitarity restrictions, we consider $W^+W^- \to W^+W^-$, where the SM contributions are shown in Fig. 1 and Fig. 2. The diagrams of Fig. 1 individually have terms that grow like s^2/M_W^4, but the sum grows only as s/M_W^2. If the $W^+W^-W^+W^-$, W^+W^-Z or $W^+W^-\gamma$ vertices were altered by the presence of the non-SM contributions in an EFT, this cancellation would be spoiled, leading to unitarity violation at some energy. The amplitudes resulting from the diagrams of Fig. 2 have terms which grow with s/M_W^2, but these terms cancel with the contributions from the diagrams of Fig. 1, leaving a result which does not grow with energy. Again, any alterations of the W^+W^-H couplings would spoil this cancellation.

We can calculate the high energy limit of the $W^+W^- \to W^+W^-$ amplitude in a simple manner using the electroweak equivalence theorem. The formal statement of the electroweak equivalence theorem is that,

$$\begin{aligned} \mathcal{A}(V_L^1 V_L^2 .... V_L^N \to V_L^1 V_L^2 .... V_L^{N'}) \;=\; & (i)^N (-i)^{N'} \mathcal{A}(\omega_1 \omega_2 ... \omega_N \to \omega_1 \omega_2 ... \omega_{N'}) \\ & + \mathcal{O}\bigg(\frac{M_V^2}{s}\bigg), \end{aligned} \tag{21}$$

where ω_i is the Goldstone boson corresponding to the longitudinal gauge boson, V_L^i. In other words, when calculating scattering amplitudes of longitudinal gauge bosons at high energy, we can replace the *external* longitudinal gauge bosons by Goldstone bosons. We note that the scattering of transverse W bosons is proportional to g^2 and contains no new features.

As a demonstration of unitarity restrictions, we consider the scattering of longitudinal gauge bosons, $W_L^+W_L^- \to W_L^+W_L^-$, which can be found to $\mathcal{O}(M_W^2/s)$ from the Goldstone

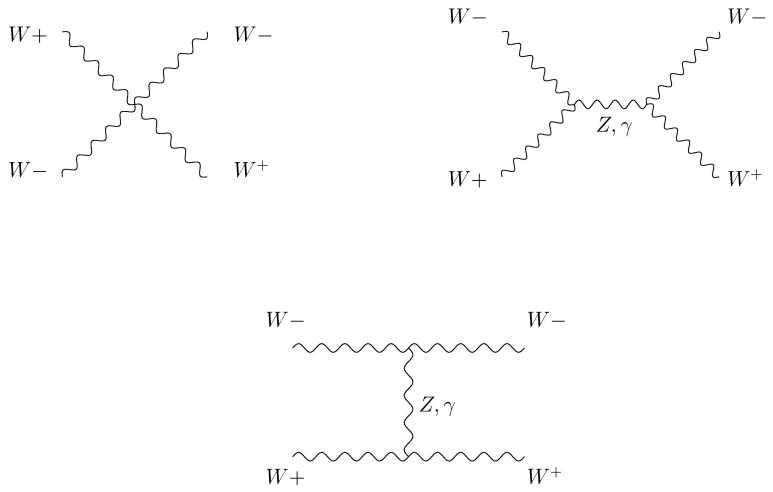

FIG. 1: WW elastic scattering contributions from 3- and 4- gauge boson couplings.

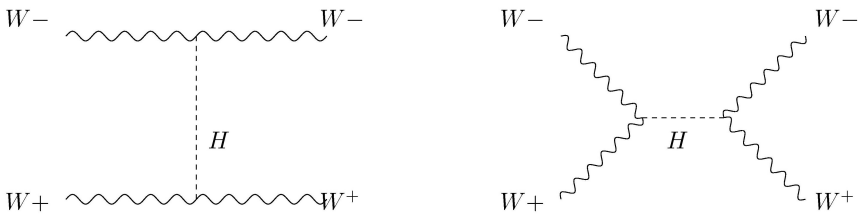

FIG. 2: WW elastic scattering from Higgs exchange.

boson scattering of Eq 21. In Feynman gauge, the three Goldstone bosons, $\omega^{\pm}, z$, have mass

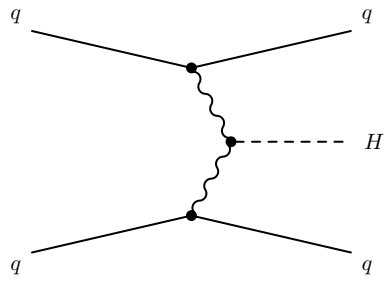

FIG. 3: Vector boson fusion scattering.

$M_{\omega,z} = M_{W,Z}$ and have the interactions[1],

$$V = \frac{M_H^2}{2v} h\left(H^2 + Z^2 + 2\omega^+\omega^-\right) + \frac{M_H^2}{8v^2}\left(H^2 + z^2 + 2\omega^+\omega^-\right)^2. \tag{22}$$

The scattering amplitude for $\omega^+\omega^- \to \omega^+\omega^-$, which agrees with $W_L^+W_L^- \to W_L^+W_L^-$, to $\mathcal{O}(M_W^2/s)$ is

$$A(\omega^+\omega^- \to \omega^+\omega^-) = -\frac{M_H^2}{v^2}\left(\frac{s}{s - M_H^2} + \frac{t}{t - M_H^2}\right). \tag{23}$$

where we include only the terms proportional to M_H^2/v^2. The diagrams are shown in Fig. **??**. It is much easier to calculate using the Goldstone bosons!

We construct the $J = 0$ partial wave, a_0^0, in the limit $M_W^2 << s$ from Eq. 23,

$$\begin{aligned} a_0^0(\omega^+\omega^- \to \omega^+\omega^-) &\equiv \frac{1}{16\pi s}\int_{-s}^{0} \mid A \mid dt \\ &= -\frac{M_H^2}{16\pi v^2}\left[2 + \frac{M_H^2}{s - M_H^2} - \frac{M_H^2}{s}\log\left(1 + \frac{s}{M_H^2}\right)\right]. \end{aligned} \tag{24}$$

If we go to very high energy, $s >> M_H^2$, then Eq. 24 has the limit,

$$a_0^0(\omega^+\omega^- \to \omega^+\omega^-) \longrightarrow_{s>>M_H^2} -\frac{M_H^2}{8\pi v^2}. \tag{25}$$

The Higgs boson therefore plays a fundamental role in the theory since it cuts off the growth of the partial wave amplitudes and makes the theory obey perturbative unitarity. A 125 GeV Higgs remains perturbative up to the Planck scale at tree level.

C. WW Scattering

WW scattering is not just of interest for unitarity considerations, but is a real process. The vector boson fusion (VBF) scattering diagram is shown in Fig. 3 Since

[1] Remember that the mass and interactions of the Goldstone bosons are gauge dependent!

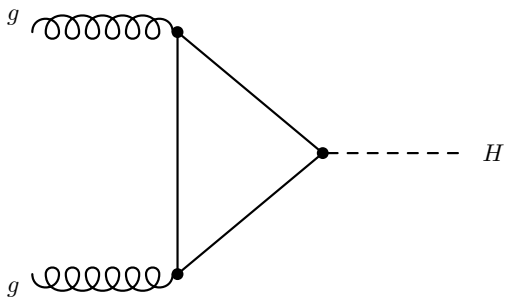

FIG. 4: Top quark contribution to the $gg \to H$ amplitude.

there is no resonance in VBF scattering, it is a counting experiment. The cross section, $\sigma(VBF)[8\ TeV = 1.6\ pb$, and is larger than naively expected. The integral of the cross section over the final state phase space has a contribution for the W boson propagator. If we define k to be the W momenta, and θ the angle between the incoming and outgoing quarks (with energies in the lab frame of E, E') emitting the W, then

$$\int \frac{d\theta}{(k^2 - M_W^2)^2} \sim \frac{d\theta}{(2EE'(1-\cos\theta) + M_W^2)^2} \tag{26}$$

There are 2 important consequences of Eq. 26. The first is that the rate is enhanced in the forward direction, and so there will be 2 forward jets that can be tagged. The second is that the rate is not suppressed at high energy, but rather,

$$\sigma \sim \frac{1}{M_W^2} \log\left(\frac{s}{M_W^2}\right). \tag{27}$$

Following the discussion in the previous sections, the measurement of VBF scattering is sensitive to non-SM gauge self-interactions and will have effects which grow with the WW invariant mass.

III. GLUONS AND THE HIGGS

A. $gg \to H$

Since the Higgs does not couple to gluons, the primary production mechanism for a Higgs boson in hadronic collisions is through the couplings to heavy fermions, $gg \to H$, which is shown in Fig. 4. This process is dominated by the top quark loop, and the loop with a bottom quark contributes roughly -5% to the cross section.

We evaluate this diagram using dimensional regularization in $n = 4 - 2\epsilon$. The amplitude for a color triplet fermion of mass m is,

$$iA^{\mu\nu} = -(-ig_s)^2 Tr(T_A T_B)\left(-\frac{m}{v}\right)\int \frac{d^n k}{(2\pi)^n}\frac{T^{\mu\nu}}{D}(i)^3\epsilon_\mu(p)\epsilon_\nu(q)\,. \tag{28}$$

The overall minus sign is due to the closed fermion loop and $\epsilon(p), \epsilon(q)$ are the transverse polarization vectors of the gluons. The denominator is $D = (k^2 - m^2)[(k+p)^2 - m^2][(k-q)^2 - m^2]$. The denominators can be combined using Feynman parameterization,

$$\frac{1}{ABC} = 2\int_0^1 dx \int_0^{1-x} \frac{dy}{[Ax + By + C(1-x-y)]^3} \tag{29}$$

which yields,

$$\frac{1}{D} \to 2\int dxdy \frac{1}{[k^2 - m^2 + 2k\cdot(px - qy)]^3}\,. \tag{30}$$

Shifting the integration momenta, $k' = k + px - qy$, the denominator becomes,

$$\frac{1}{D} \to 2\int dxdy \frac{1}{[k'^2 - m^2 + M_H^2 xy]^3} \tag{31}$$

The numerator of Eq. 28 after the shift of momentum is,

$$\begin{aligned} T^{\mu\nu} \;=\; & 4m\Bigg\{ g^{\mu\nu}\left[m^2 - k'^2 + M_H^2(xy - \frac{1}{2})\right] \\ & +4k'^\mu k'^\nu + p^\nu q^\mu(1 - 4xy)\Bigg\}\,, \end{aligned} \tag{32}$$

where we note that gauge invariance requires $p\cdot A^{\mu\nu} = q\cdot A^{\mu\nu} = 0$. The integral can be symmetrized, $k'^\mu k'^\nu \to g^{\mu\nu}\frac{k'^2}{n}$, giving the amplitude,

$$\begin{aligned} iA \;=\; & -\frac{2g_s^2 m^2}{v}\delta_{AB}\int \frac{d^n k'}{(2\pi)^n}\Bigg\{ g^{\mu\nu}\left[m^2 + k'^2\left(\frac{4}{n} - 1\right) + M_H^2(xy - \frac{1}{2})\right] \\ & +p^\nu q^\mu(1 - 4xy)\Bigg\}\frac{2dxdy}{[k'^2 - m^2 + M_H^2 xy]^3}\epsilon_\mu(p)\epsilon_\nu(q)\,. \end{aligned} \tag{33}$$

The integrals of Eq. 33 are well known,

$$\begin{aligned} \int \frac{d^n k'}{(2\pi)^n}\frac{k'^2}{[k'^2 - C]^3} \;&=\; \tfrac{i}{32\pi^2}(4\pi)^\epsilon \tfrac{\Gamma(1+\epsilon)}{\epsilon}(2-\epsilon)C^{-\epsilon} \\ \int \frac{d^n k'}{(2\pi)^n}\frac{1}{[k'^2 - C]^3} \;&=\; -\tfrac{i}{32\pi^2}(4\pi)^\epsilon \tfrac{\Gamma(1+\epsilon)}{\epsilon}C^{-1-\epsilon} \end{aligned} \tag{34}$$

Putting it all together, (and inserting a factor of 2 to include the crossed diagram), we find the amplitude,

$$\begin{aligned} A^{\mu\nu}(gg \to H) &= -\frac{\alpha_s m^2}{\pi v}\delta_{AB}\left(g^{\mu\nu}\frac{M_H^2}{2} - p^\nu q^\mu\right) \\ &\quad \cdot \int_0^1 dx \int_0^{1-x} dy \left(\frac{1-4xy}{m^2 - M_H^2 xy}\right)\epsilon_\mu(p)\epsilon_\nu(q) \\ &= -\frac{\alpha_s}{4\pi v}\delta_{AB}\left(g^{\mu\nu}\frac{M_H^2}{2} - p^\nu q^\mu\right)F_{1/2}(\tau)\epsilon_\mu(p)\epsilon_\nu(q) \\ &\to -\frac{\alpha_s}{3\pi v}\delta_{AB}\left(g^{\mu\nu}\frac{M_H^2}{2} - p^\nu q^\mu\right)\epsilon_\mu(p)\epsilon_\nu(q) \qquad \text{if } m >> M_H\,, \end{aligned} \tag{35}$$

and

$$\begin{aligned} F_{1/2}(\tau) &= 4\int_0^1 dx \int_0^{1-x} dy \left(\frac{1-4xy}{1-4\tau xy}\right) \\ &= \frac{2}{\tau^2}\Big[\tau + (\tau-1)f(\tau_t)\Big] \\ f(\tau) &= \left(\sin^{-1}(\sqrt{\tau})\right)^2 \qquad \text{if } \tau \le 1 \\ &= -\frac{1}{4}\left[\ln\left(\frac{1+\sqrt{1-1/\tau}}{1-\sqrt{1-1/\tau}}\right) - i\pi\right]^2 \qquad \text{if } \tau > 1 \end{aligned} \tag{36}$$

and $\tau_t = \frac{M_H^2}{4m^2}$. Note that $F_{1/2}(\tau) \to \frac{4}{3}$ as $\tau \to 0$ and the function quickly approaches its asymptotic value. On the other hand, the contribution of a light quark such as the b vanishes as $m_b^2 \log\left(\frac{m_b^2}{M_H^2}\right)$ and so it is only the heavy quarks that are important for the $gg \to H$ process.

The tensor structure of Eq. 35 is exactly that required for the production of a spin-0 particle. Suppose we start from a $G_{\mu\nu}G^{\mu\nu}$ term in the Lagrangian and consider only the Abelian contributions for now,

$$G_{\mu\nu}G^{\mu\nu} \to (\partial_\mu G_\nu - \partial_\nu G_\mu)(\partial^\mu G^\nu - \partial^\nu G^\mu)\,. \tag{37}$$

Making the replacement $\partial_\mu \to ik_\mu$,

$$\begin{aligned} G_{\mu\nu}G^{\mu\nu} &\to -(k_{1\mu}G_{1\nu} - k_{1\nu}G_{1\mu})(k_2^\mu G_2^\nu - k_2^\nu G_2^\mu) \\ &= -2\Big(k_1\cdot k_2 G_1\cdot G_2 - k_1\cdot G_2 k_2\cdot G_1\Big) \\ &= -2k_1\cdot k_2 G_{1\mu}G_{2\nu}\left[g^{\mu\nu} - \frac{k_1^\nu k_2^\mu}{k_1\cdot k_2}\right]. \end{aligned} \tag{38}$$

Comparing Eq. 33 and 38 suggests that the heavy quark limit for gluon fusion can be obtained from the effective Lagrangian[2]

$$L^t_{EFT} = \frac{\alpha_s}{12\pi}\frac{h}{v}G^A_{\mu\nu}G^{\mu\nu A}\,. \tag{39}$$

The cross section can be found from the general resonance formula,

$$\hat{\sigma}(gg \to H) = \frac{16\pi^2}{M_H}(2J+1)\frac{1}{64}\cdot\frac{1}{4}\cdot 2\Gamma(H\to gg)\delta(s-M_H^2)\,, \tag{40}$$

where the factors of $\frac{1}{64}$ and $\frac{1}{4}$ are the color and spin averages, $J=0$ is the Higgs spin, and the factor of 2 undoes the identical particle factor of $\frac{1}{2}$ in the decay width $\Gamma(H\to gg)$. The lowest order cross section for $gg\to h$ is then,

$$\begin{aligned}\hat{\sigma}(gg\to h) &= \frac{\alpha_s^2}{1024\pi v^2}\mid\sum_q F_{1/2}(\tau_q)\mid^2\delta\left(1-\frac{s}{M_H^2}\right)\\ &\equiv \hat{\sigma}_0(gg\to h)\delta\left(1-\frac{s}{M_H^2}\right)\quad,\end{aligned} \tag{41}$$

where s is the gluon-gluon sub-process center of mass energy. In the heavy quark limit, the cross section becomes a constant,

$$\hat{\sigma}_0(gg\to h)\sim\frac{\alpha_s^2}{576\pi v^2}\quad. \tag{42}$$

The heavy fermions do not decouple–this is because particles whose couplings are proportional to mass do not satisfy the criteria for the decoupling theorem to apply.

The Higgs boson production cross section at a hadron collider can be found by integrating the parton cross section, $\sigma_0(pp\to h)$, with the gluon parton distribution functions, $g(x)$,

$$\sigma(pp\to h) = \hat{\sigma}_0 z\int_z^1\frac{dx}{x}g(x)g\left(\frac{z}{x}\right), \tag{43}$$

where σ_0 is given in Eq. 41, $z\equiv M_H^2/S$, and S is the hadronic center of mass energy. At the LHC, $\sigma(pp\to H)[8\ TeV] = 19\ pb$ and $\sigma(pp\to H)[13\ TeV] = 44\ pb$, where these theoretical numbers include large radiative corrections to the lowest order rate.

B. Implications of $gg\to H$

The measured Higgs rate immediately rules out the possibility of a $4th$ generation of SM chiral fermions. Imagine that there are heavy fermions, $\mathcal{T}$ and $\mathcal{B}$, with the identical quantum

[2] The extra factor of $\frac{1}{2}$ comes from the neglected color factor, $Tr(T_AT_B) = \frac{1}{2}\delta_{AB}$.

numbers as the SM top and bottom. Then they would contribute to Higgs production from gluon fusion as in Fig. 4. From Eq. 42, we would have,

$$\begin{aligned}\hat{\sigma}_0(gg \to h) &\to \frac{\alpha_s^2}{576\pi v^2}\left[1+1+1\right]^2 \\ &\to 9\hat{\sigma}_0(SM)\,,\end{aligned} \tag{44}$$

where the factors in the square bracket represent the contributions of $t, \mathcal{T}$ and $\mathcal{B}$. This is obviously excluded by the measured rate for gluon fusion Higgs production, which is in good agreement with the SM prediction.

This does not mean that all heavy fermions are excluded however. Vector-like fermions do not have large contributions to the Higgs rate. The simplest possibility is to add a fermionic top partner, T, for which both the left- and right- handed components are weak singlets and color triplets[3]. In this scenario, the top partner can have a Dirac mass, (which has nothing to do with electroweak symmetry breaking), and can mix with the SM top quark. The most general Yukawa interaction is,

$$-L_Y \;\sim\; \lambda_t \overline{q}_L \tilde{\Phi} t_R + \lambda_2 \overline{q}_L \tilde{\Phi} T_R + \lambda_3 \overline{T}_L t_R + \lambda_4 \overline{T}_L T_R\,. \tag{45}$$

The physical charge- $\frac{2}{3}$ particles, t_1 and t_2, are mixtures of t and T,

$$\begin{aligned} t_{1(L,R)} &= \cos\theta_{L,R} t_{L,R} - \sin\theta_{L,R} T_{L,R} \\ t_{2(L,R)} &= \sin\theta_{L,R} t_{L,R} + \cos\theta_{L,R} T_{L,R}\,, \end{aligned} \tag{46}$$

where the mixing angles can be determined in terms of the parameters of the potential. The important point is that the couplings to the Higgs boson are changed in models with vector-like fermions,

$$\begin{aligned} L_H \;=\; & -\frac{m_{t1}}{v}\cos^2\theta_L \bar{t}_{1,L} t_{1,R} h - \frac{m_{t2}}{v}\sin^2\theta_L \bar{t}_{2,L} t_{2,R} h \\ & -\frac{m_{t2}}{v}\cos\theta_L \sin\theta_L \bar{t}_{1,L} t_{2,R} h - \frac{m_{t1}}{v}\cos\theta_L \sin\theta_L \bar{t}_{2,L} t_{1,R} + h.c. \end{aligned} \tag{47}$$

In the large mass limit, the top and top partner contributions to gluon fusion yield

$$\begin{aligned}\hat{\sigma}_0(gg \to h) &\to \frac{\alpha_s^2}{576\pi v^2}\left[\cos^2\theta_L + \sin^2\theta_L\right]^2 \\ &\to \hat{\sigma}_0(SM)\,,\end{aligned} \tag{48}$$

[3] Note that left- and right-handed fermions contribute with opposite signs to anomalies and so the contributions cancel. Therefore, it is not required to have a full generation of vector-like fermions to cancel anomalies.

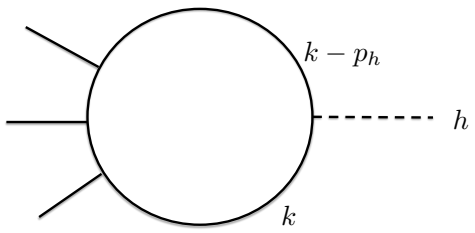

FIG. 5: General Higgs coupling to fermions.

This equivalence with the SM gluon fusion rate in models with vector- like fermions is a general feature.

C. Gluon Fusion and Low Energy Theorems

The idea that the Higgs couplings to heavy particles can be derived from an effective Lagrangian as in Eq. 39 gives rise to low energy theorems that are quite general. Consider the Higgs coupling to a heavy fermion as part of a complicated Feynman diagram as shown in Fig. 5. This amplitude can be written in the limit $p_H \to 0$ as,

$$\begin{aligned}(...)\frac{i}{k-m}\frac{-im}{v}\frac{i}{k-p_h-m}(...) \;&\to\; (...)\frac{i}{m}\left(\frac{1}{k-m}\right)^2(....) \\ &=\; (...)\frac{im}{v}\frac{\partial}{m}\left(\frac{1}{k-m}\right)(...)\,. \end{aligned} \tag{49}$$

In complicated diagrams, the combinatorics works out correctly.

This has been formalized to a theorem,

$$lim(p_h \to 0)A(HX) = \frac{m}{v}\frac{\partial}{\partial m}A(X)\,, \tag{50}$$

that is, adding a Higgs boson to a diagram is equivalent to taking the derivative with respect to the heavy fermion mass[4]. It is important to note that the derivative is with respect to

[4] Identical reasoning holds for the coupling of a Higgs boson to gauge bosons.

the unrenormalized mass. At higher orders, there are contributions from $\partial m_R/\partial m$, where m_R is the renormalized mass.

Let us apply Eq. 50 to the gluon 2-point function,

$$L = -\frac{1}{4g_s^2} G'^A_{\mu\nu} G'^{\mu\nu A}\,, \tag{51}$$

where we have factored all coupling constant dependence out of $G' = \frac{G}{g_s}$ for convenience. We apply the low energy theorem,

$$L^t_{EFT} = -\frac{1}{4}\frac{h}{v}\left[m\frac{\partial}{\partial m}\frac{1}{g_s^2}\right] G'^A_{\mu\nu} G'^{\mu\nu A}\,, \tag{52}$$

and remember that,

$$\beta = \mu\frac{\partial g_s}{\partial \mu}\,. \tag{53}$$

Noting that only the heavy top quark contributes here,

$$\frac{\beta}{g_s} \to \frac{\alpha_s}{6\pi}\,, \tag{54}$$

and the low energy theorem of Eq. 39 is reproduced.

The low energy theorem is more than just a curiosity. The EFT of Eq. 39 has been used to calculate radiative corrections to Higgs production at NLO, NNLO, and NNNLO. For the NLO corrections to $gg \to H$, the 2-loop virtual corrections in the full theory become 1-loop calculations using the EFT and so on. This greatly reduces the complexity of the problem. At NNLO, the validity of the EFT has been checked numerically in the exact top mass dependent theory by expanding the propagators in the large mass limit, and the agreement is within a few percent. Practically speaking, the higher order results obtained using the EFT are typically rescaled by the LO results including the full top quark mass dependence.

At LO, the Higgs boson has no p_T. Transverse momentum for the Higgs is first generated by the process, $gg \to gh$. Radiative corrections to this process have also been calculated using the EFT, but here there are more momentum scales. The expansion in $\frac{M_H}{m_t}$ receives contributions of $\mathcal{O}\left(\frac{s}{m_t^2}\right)$, and so care needs to be taken.

D. Low Energy Theorems and Beyond the SM Physics

The low energy theorems described in the previous section are valuable for calculating radiative corrections to Higgs production in the SM, but they can also be used in BSM

models with heavy non-SM colored particles. Consider, for example, a model with many fermions, $\mathcal{F}_i$, with the interactions in the mass basis,

$$L \sim \Sigma_i \overline{\mathcal{F}}_i \tilde{Y}_i (h+v) \mathcal{F}_i \,, \tag{55}$$

with $m_i = v\tilde{Y}_i$ Then the obvious generalization of the results of the previous section is,

$$L_{EFT} = \frac{\alpha_s}{12\pi} h \Sigma_i \frac{\tilde{Y}_i}{m_i} G^A_{\mu\nu} G^{\mu\nu A} \,. \tag{56}$$

In general, however, the fermion-Higgs couplings are specified in the gauge basis, and it is quite a bit of work to obtain the mass basis. This step can be eliminated using the low energy theorems. Start from the general interactions of the fermions in the gauge basis, and diagonalize the mass matrix, M, using the unitary matrix, U, where $M_D = U^\dagger M U$,

$$\begin{aligned} L \;&\sim\; \Sigma_{ij} \overline{f}_i Y_{ij} (h+v) f_j \\ &=\; \overline{f} U U^\dagger Y U U^\dagger f (h+v) \,, \end{aligned} \tag{57}$$

where the diagonal mass matrix is $M_D = v U^\dagger Y U$ and $M = Yv$ (and M, M_D, $\tilde{Y}$ and Y are now all interpreted as matrices). The Higgs couplings to gluons are determined,

$$\begin{aligned} R_g \;&\equiv\; \Sigma_i \frac{\tilde{Y}_i}{m_i} \\ &=\; \Sigma_i \left(\frac{U^\dagger Y U}{m} \right)_{ii} = Tr(U^\dagger Y U M_D^{-1}) = Tr(Y U M_D^{-1} U^\dagger) \,. \end{aligned} \tag{58}$$

Now use the matrix identity $M^{-1}M = M^{-1} U M_D U^\dagger = 1$, and

$$\begin{aligned} R_g \;&=\; Tr(Y [M^{-1} U M_D U^\dagger][U M_D^{-1} U^\dagger]) \\ &=\; Tr(Y M^{-1}) \\ &=\; Tr\left(\frac{\partial M}{\partial v} M^{-1} \right) \\ &=\; \frac{\partial}{\partial v} \log(detM)) \\ &=\; \frac{\partial}{\partial v} Tr(log(M) \,, \end{aligned} \tag{59}$$

where in the last 2 lines we have used some nifty matrix identities. The effective Lagrangian is now given by,

$$L_{EFT} = \frac{\alpha_s}{12\pi} \frac{h}{v} \left(\frac{\partial}{\partial \log(v)} Tr(logM) \right) G^A_{\mu\nu} G^{\mu\nu A} \,, \tag{60}$$

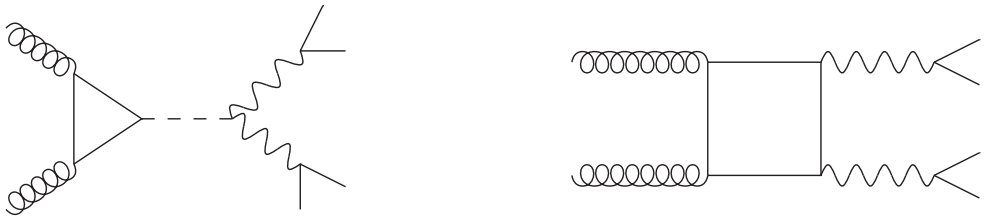

FIG. 6: Contributions to $gg \to ZZ \to 4l$. The dominant contributions to the triangle and box are from the top quark.

and there is no need to diagonalize the mass matrix.

We can also consider the general EFT for the higgs couplings to gluons, where Λ is some high scale, $\Lambda >> v$

$$L \sim L_{SM} + \frac{\alpha_s}{12\pi}\frac{c_g}{\Lambda^2}(\Phi^\dagger\Phi)G^A_{\mu\nu}G^{\mu\nu A} - \left(\frac{c_t}{\Lambda^2}\overline{q}_L\tilde{\Phi}q_R(\Phi^\dagger\Phi) + h.c.\right). \tag{61}$$

This formulation assumes that the Higgs is an $SU(2)$ doublet and so only $SU(2)$ invariant terms are considered. This commonly used EFT looks similar to Eq. 39, but Eq. 61 is actually different. In this formulation, top quark effects are included exactly in L_{SM} and in the SM limit, $c_g = c_t = 0$. In the heavy mass limit, the result including new BSM physics is,

$$A(gg \to H) = A(gg \to H)\left(1 + \frac{v^2}{\Lambda^2}(c_g + c_t)\right), \tag{62}$$

and so gluon fusion cannot distinguish between c_g and c_t.

E. Measuring the Higgs width with $gg \to H \to ZZ$

The total SM Higgs width is $\Gamma_H \sim 4\ MeV$ which is found by adding up the predictions for all the SM decays and assuming there are no undetected or invisible decays. Making a direct measurement by looking for the resonance $H \to \gamma\gamma$ or $H \to ZZ$ is not possible since the detector resolution is $\mathcal{O}(1 - 2\ GeV)$, much larger than the Higgs width.

A clever idea uses the properties of the longitudinal Z polarizations. Consider the process $gg \to ZZ \to 4l$ shown in Fig. 6. The Higgs contribution is shown on the LHS of Fig. 6 and the partonic cross section from the Higgs contribution alone is generically given by,

$$\hat{\sigma}(gg \to H \to ZZ) \sim \int ds \frac{\mid A(gg \to H \to ZZ) \mid^2}{(s - M_H^2)^2 + \Gamma_H^2 M_H^2}. \tag{63}$$

We allow the effective $gg \to H$ and $ZZ \to H$ couplings to be scaled by arbitrary factors $\kappa_g(s)$ and $\kappa_Z(s)$, where we explicitly note that the κ factors can in principle depend on scale,

$$\mid A(gg \to H \to ZZ) \mid^2 \sim \kappa_g^2(s)\kappa_Z^2(s) \mid \epsilon_{Z1} \cdot \epsilon_{Z2} \mid^2 \tag{64}$$

The interesting observation is that Eq. 63 behaves very differently above the Higgs resonance and near the resonance. Above the resonance, $s >> M_H^2$, Eq. 63 becomes,

$$\hat{\sigma}(gg \to H \to ZZ)^{above} \sim \int ds \frac{\kappa_g^2(s)\kappa_Z^2(s) \mid \epsilon_{Z1} \cdot \epsilon_{Z2} \mid^2}{s^2} \,. \tag{65}$$

For transverse polarizations, nothing particularly new happens, but because of the electroweak symmetry breaking the longitudinal polarization has an interesting feature. Defining the momenta of the outgoing Z bosons as p_{Z1} and p_{Z2} and remembering that the longitudinal polarization is approximately given by,

$$\epsilon_L^\mu(p_Z) \sim \frac{p_Z^\mu}{M_Z} + \mathcal{O}\left(\frac{M_Z^2}{s}\right), \tag{66}$$

Eq. 65 has the approximate form,

$$\hat{\sigma}(gg \to H \to Z_L Z_L)^{above} \sim \int ds \frac{\kappa_g^2(s)\kappa_Z^2(s)}{M_Z^4} \,. \tag{67}$$

Near the Higgs resonance, we can use the narrow width approximation, which amounts to the replacement,

$$\frac{1}{(s - M_H^2)^2 + (M_H\Gamma_H)^2} \to \frac{\pi}{M_H\Gamma_H}\delta(s - M_H^2) \tag{68}$$

and Eq. 63 is approximately,

$$\hat{\sigma}(gg \to H \to ZZ)^{on} \sim \frac{\kappa_g^2(M_H^2)\kappa_Z^2(M_H^2)}{M_H\Gamma_H} \,. \tag{69}$$

The idea is that by measuring the $gg \to H \to ZZ$ rate above and on the resonance, information can be extracted about the Higgs width. Assuming the κ factors do not depend on scale,

$$\Gamma_h \sim \frac{\hat{\sigma}^{above}}{\hat{\sigma}^{on}} \,. \tag{70}$$

At 8 TeV, approximately 15% of the cross section has $m_{4l} > 140$ GeV, so this is a promising idea. If the κ factors have an energy dependence, they do not cancel in Eq. 70 and the interpretation of the measurement becomes more complicated.

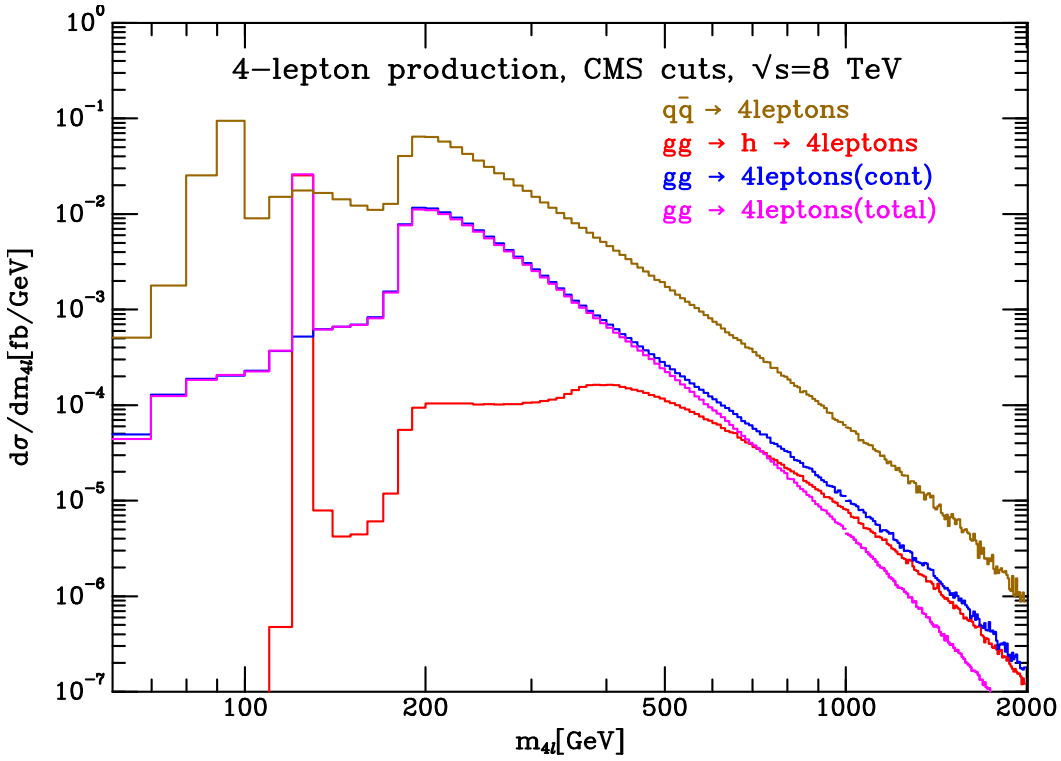

FIG. 7: Contributions to $gg \to ZZ \to 4l$ at 8 TeV. The Higgs contributions are shown in red, while the total rate from gluon fusion including interference is given in magenta[1].

Of course, a real calculation needs to include both the diagrams of Fig. 6, along with the interference, and this has been done by several groups with results shown in Fig. 7. The importance of including the interference terms is apparent, but the long tail at high m_{4l} (shown in red) is clear. ATLAS and CMS have used this technique to place limits on the Higgs width,

$$\Gamma_H < (4-5)\Gamma_H^{SM} \,. \tag{71}$$

There are some big assumptions in this extraction of the Higgs width, the most obvious of which is the assumption that the κ factors are the same on and off the peak. This is clearly a false assumption, since in a quantum field theory all couplings run. If there are anomalous HZZ (or Hgg) couplings, than the running could be changed significantly. For example, a contribution to the EFT of the form,

$$L \sim \frac{c_Z}{\Lambda^2}\frac{H}{v} Z_{\mu\nu} Z^{\mu\nu} \tag{72}$$

would give contributions of $\mathcal{O}\left(\frac{s}{\Lambda^2}\right)$ and would cause m_{4l} to grow above the peak, and would

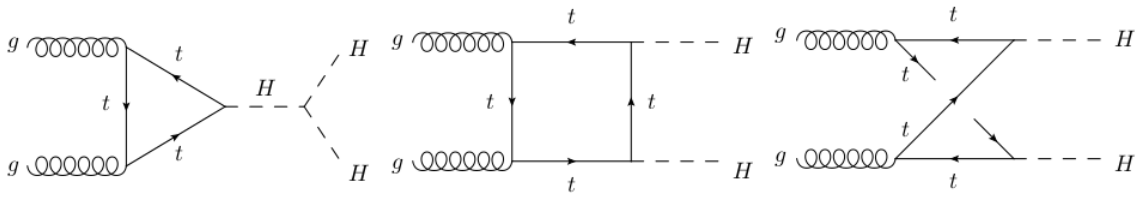

FIG. 8: Contributions to $gg \to HH$. The dominant contribution to the triangle and box is from the top quark.

invalidate the extraction of Γ_h.

It is worth noting that an e^+e^- collider with an energy of $\sqrt{s} = 500\ GeV$ can make a 5% measurement of Γ_H with an integrated luminosity of 500 GeV. First the measurement of $e^+e^- \to ZH$ is made by tagging the ZH events where the recoil mass is consistent with a Higgs boson. This is done using conservation of momenta and determines $\sigma(ZH)$. Now measure the $H \to ZZ$ rate to determine $BR(H \to ZZ)$. The Higgs width is then determined,

$$\begin{aligned} \Gamma_H &= \Gamma(H \to ZZ) BR(H \to ZZ) \\ &\sim \frac{\sigma(ZH)}{BR(H \to ZZ)} \,. \end{aligned} \tag{73}$$

F. Double Higgs Production

Finally, we would like to measure the parameters of the Higgs potential to determine if electroweak symmetry breaking really proceeds as in the SM. In the SM, the Higgs potential is

$$\begin{aligned} V &= \mu^2 \Phi^\dagger \Phi + \lambda (\Phi^\dagger \Phi)^2 \\ &= \frac{M_H^2}{2} H^2 + \frac{M_H^2}{2v} H^3 + \frac{M_H^2}{8v^2} H^4 \\ &= \frac{M_H^2}{2} H^2 + \lambda_3 H^3 + \lambda_4 H^4 \,. \end{aligned} \tag{74}$$

It is important to verify that the λ_3 and λ_4 couplings have the vlaues predicted by the SM.

The only way to directly probe the H^3 coupling is by double Higgs production which proceeds through the diagrams of Fig. 8. The result is sensitive to new colored particles in the loops and to the Higgs trilinear self-coupling. The amplitude for $g^{A,\mu}(p_1) g^{B,\nu}(p_2) \to$

$H(p_3)H(p_4)$ is,

$$A^{\mu\nu}_{AB} = \frac{\alpha_s}{8\pi v^2}\delta_{AB}\left[P_0^{\mu\nu}(p_1,p_2)F_1(s,t,u,m_t^2) + P_2^{\mu\nu}(p_1,p_2,p_3)F_2(s,t,u,m_t^2)\right] , \qquad (75)$$

where P_0 and P_2 are the orthogonal projectors onto the spin-0 and spin-2 states respectively,

$$\begin{aligned} P_0^{\mu\nu}(p_1,p_2) &= g^{\mu\nu} - \frac{p_1^\nu p_2^\mu}{p_1\cdot p_2} , \\ P_2^{\mu\nu}(p_1,p_2,p_3) &= g^{\mu\nu} + \frac{2}{s p_T^2}\left(M_H^2 p_1^\nu p_2^\mu - 2p_1.p_3\, p_2^\mu p_3^\nu - 2p_2.p_3\, p_1^\nu p_3^\mu + s\, p_3^\mu p_3^\nu\right) , \end{aligned} \qquad (76)$$

s, t, and u are the partonic Mandelstam variables, $s = (p_1+p_2)^2, t = (p_1-p_3)^2, u = (p_2-p_3)^2$, and p_T is the transverse momentum of the Higgs particle,

$$p_T^2 = \frac{ut - M_H^4}{s} . \qquad (77)$$

The functions F_1 and F_2 are known analytically [2, 3].

In the Standard Model, the dominant contributions come from top quark loops. In the limit $m_t^2 >> s$, the leading terms are,

$$\begin{aligned} F_1(s,t,u,m_t^2) &\equiv F_1^{tri}(s,t,u,m_t^2) + F_1^{box}(s,t,u,m_t^2) , \\ F_1^{tri}(s,t,u,m_t^2) &= \frac{4M_H^2}{s-M_H^2}s\left\{1 + \frac{7}{120}\frac{s}{m_t^2} + \frac{1}{168}\frac{s^2}{m_t^4} + \mathcal{O}\left(\frac{s^3}{m_t^6}\right)\right\} , \\ F_1^{box}(s,t,u,m_t^2) &= -\frac{4}{3}s\left\{1 + \frac{7}{20}\frac{M_H^2}{m_t^2} + \frac{90M_H^4 - 28M_H^2 s + 12s^2 - 13p_T^2 s}{840m_t^4} + \mathcal{O}\left(\frac{s^3}{m_t^6}\right)\right\} ; \\ F_2(s,t,u,m_t^2) &= -\frac{11}{45}s\frac{p_T^2}{m_t^2}\left\{1 + \frac{62M_H^2 - 5s}{154m_t^2} + \mathcal{O}\left(\frac{s^2}{m_t^4}\right)\right\} . \end{aligned} \qquad (78)$$

It is well known that the expansion in powers of $1/m_t$ poorly reproduces kinematic distributions, due to the presence of contributions proportional to s/m_t^2.

If we rescale the H^3 term by a factor $\delta_3 \equiv \frac{\lambda_3}{\lambda_{3,SM}}$, the leading contributions are,

$$\begin{aligned} F_1(s,t,u,m_t^2) &\to -\frac{4s}{3}\left(1 - \frac{3M_H^2\delta_3}{s-M_H^2}\right) , \\ F_2(s,t,u,m_t^2) &\to 0 . \end{aligned} \qquad (79)$$

At threshold, the box and triangle diagrams cancel, making the dependence on the H^3 coupling even more difficult to observe.

The current ATLAS limit from the 8 TeV data is $\delta_3 < 70$, which still leaves us a way to go. The rate for double Higgs production is $\sigma(pp \to HH)[13\ TeV] = 34\ fb$ and ATLAS estimates that a luminosity of 3 ab^{-1} will be sensitive to $\delta_3 > 8.7$ and $\delta_3 < -1.3$. This is

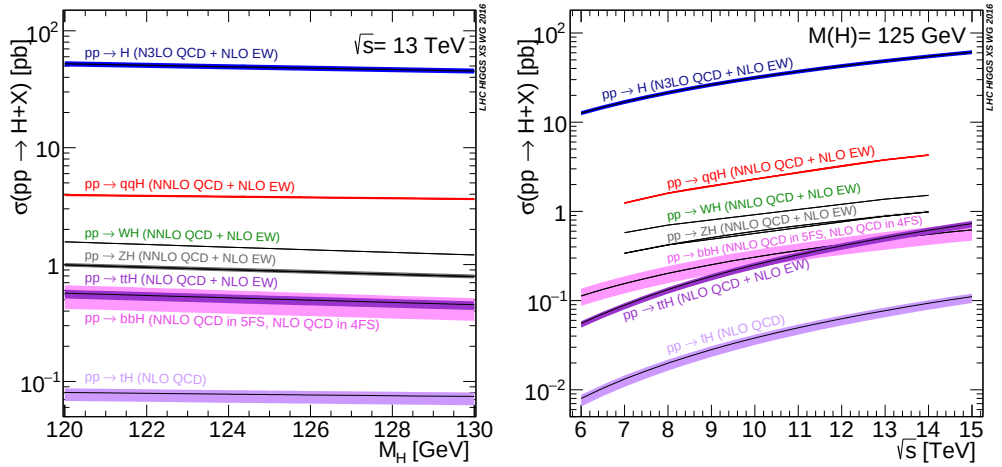

FIG. 9: Production rates for a SM Higgs boson.

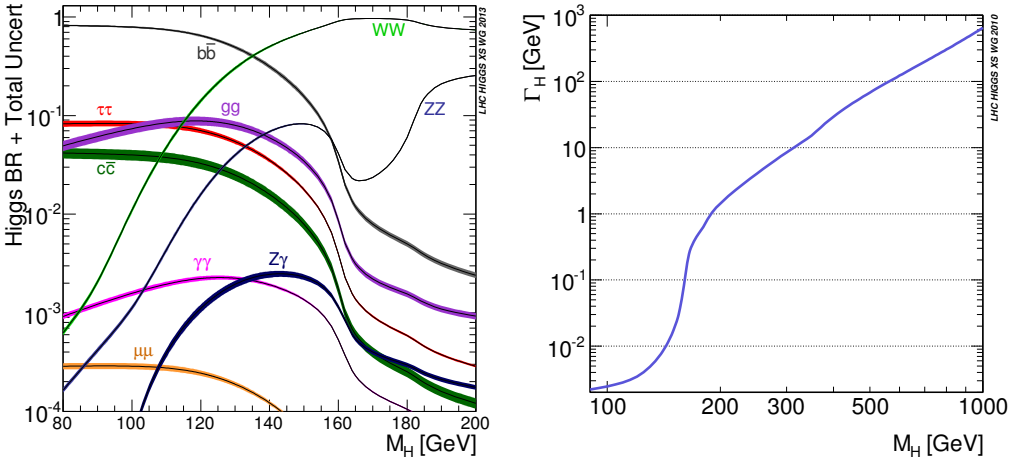

FIG. 10: Higgs branching ratio and total width.

clearly not the precision measurement we desire and the need to measure the double Higgs rate is one of the major motivations for a 100 TeV collider. Since the rate is so small, however, double Higgs production is quite sensitive to resonant effects from new physics.

IV. SM HIGGS PLOTS

In this section, we collect some useful SM results. Fig. 9 has the contributions to Higgs production from different mechanisms and Fig. 11 has the Higgs branching ratios and total width.

Also of importance are the indirect fits to M_W and m_t shown in Fig.**??**.

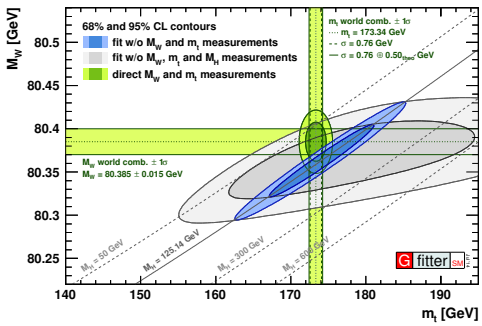

FIG. 11: Indirect limits from Gfitter.

---

[1] John M. Campbell, R. Keith Ellis, and Ciaran Williams. Bounding the Higgs width at the LHC using full analytic results for $gg- > e^-e^+\mu^-\mu^+$. *JHEP*, 04:060, 2014.

[2] E. W. Nigel Glover and J. J. van der Bij. HIGGS BOSON PAIR PRODUCTION VIA GLUON FUSION. *Nucl. Phys.*, B309:282–294, 1988.

[3] T. Plehn, M. Spira, and P. M. Zerwas. Pair production of neutral Higgs particles in gluon-gluon collisions. *Nucl. Phys.*, B479:46–64, 1996. [Erratum: Nucl. Phys.B531,655(1998)].